

## 213029: quartz–muscovite schist, GD5 Bore (Browns Range Metamorphics, Granites–Tanami Orogen)

### Location and sampling

GORDON DOWNS (SE 52-10), GORDON DOWNS (4660)  
MGA Zone 52, 495205E 7917118N

Sampled on 16 September 2013

This sample was collected from an outcrop on Gordon Downs Station, about 17.4 km south-southeast of Pussycat Bore, 16.0 km east-southeast of GD5 Bore, and 4.8 km west of the Western Australia – Northern Territory border.

### Tectonic unit/relations

The unit sampled is a quartz–muscovite schist of the Browns Range Metamorphics of the Granites–Tanami Orogen. The Browns Range Metamorphics consists mainly of amphibolite to granulite facies meta-arkose, metasandstone, and schist. The unit is unconformably overlain by the 1735–1640 Ma Gardiner Sandstone of the Birrindudu Group (Blake et al., 2000; Dunster and Ahmat, 2013). The sample was collected from the northwestern margin of the Browns Range Dome, where an arkosic metasandstone of the Browns Range Metamorphics yielded a maximum depositional age of  $2507 \pm 22$  Ma (Page et al., 1995). Another quartz–muscovite schist at this locality yielded a maximum depositional age of  $3146 \pm 7$  Ma (GSWA 213028, Lu et al., 2017b). A quartz arenite of the Gardiner Sandstone, sampled about 33 km to the west, yielded a maximum depositional age of  $1597 \pm 25$  Ma (GSWA 213019, Lu et al., 2017a)..

### Petrographic description

The sample is a quartz–muscovite schist, consisting of about 80% quartz, 10% muscovite, 7% micaceous patches, 2% opaque minerals, and accessory apatite and zircon. Quartz grains are equant to mostly elongate with some lenticular quartz up to 5 mm long. Quartz is recrystallized to polycrystalline aggregates, most of which have irregular and interdigitating shapes and remnant undulose extinction. Very fine-grained micaceous patches, up to 1 mm long, may represent replacement of either original cordierite or feldspar. Muscovite defines the strong foliation, and occurs in subparallel aggregates of highly elongate laths mostly  $>2$  mm long and 0.1 mm wide. Opaque minerals are fine-grained and fibrous, and form scaly masses associated with micaceous patches. Apatite is tabular and up to 0.2 mm long. The irregular shapes of recrystallized quartz suggest that recrystallization occurred

mainly by grain boundary migration at moderate to high metamorphic grade. The high quartz content suggests that the protolith was a quartz-rich sedimentary rock.

### Zircon morphology

Zircons isolated from this sample are colourless to dark brown, anhedral to subhedral, and variably rounded. The crystals are up to 300  $\mu\text{m}$  long, and equant to elongate, with aspect ratios up to 3:1. In cathodoluminescence (CL) images, some zircons exhibit concentric zoning, but most are dominated by high-U, metamict zones and domains. A CL image of representative zircons is shown in Figure 1.

### Analytical details

This sample was analysed on 11–13 February 2016 using SHRIMP-A. Twenty-two analyses of the BR266 standard were obtained during the session, of which 20 analyses indicated an external spot-to-spot (reproducibility) uncertainty of 0.54% ( $1\sigma$ ) and a  $^{238}\text{U}/^{206}\text{Pb}^*$  calibration uncertainty of 0.16% ( $1\sigma$ ). Isotopic mass fractionation of  $^{207}\text{Pb}/^{206}\text{Pb}$  ratios during the session was corrected by reference to the OGC1 standard; measured ratios were increased by 0.54%. Calibration uncertainties are included in the errors of  $^{238}\text{U}/^{206}\text{Pb}^*$  ratios and dates listed in Table 1. Common-Pb corrections were applied to all analyses using contemporaneous isotopic compositions determined according to the model of Stacey and Kramers (1975).

### Results

Thirty-two analyses were obtained from 32 zircons. Results are listed in Table 1, and shown in a concordia diagram (Fig. 2), and a probability density diagram (Fig. 3).

### Interpretation

The analyses are concordant to strongly discordant (Fig. 2). Twenty analyses are  $>5\%$  discordant. The dates obtained from these 20 analyses (Group D; Table 1) are unreliable, and are considered not to be geologically significant. The remaining 12 analyses can be divided into two groups, based on their  $^{207}\text{Pb}^*/^{206}\text{Pb}^*$  ratios.

Group Y comprises one analysis (Table 1), which yields a  $^{207}\text{Pb}^*/^{206}\text{Pb}^*$  date of  $2128 \pm 30$  Ma ( $1\sigma$ ).

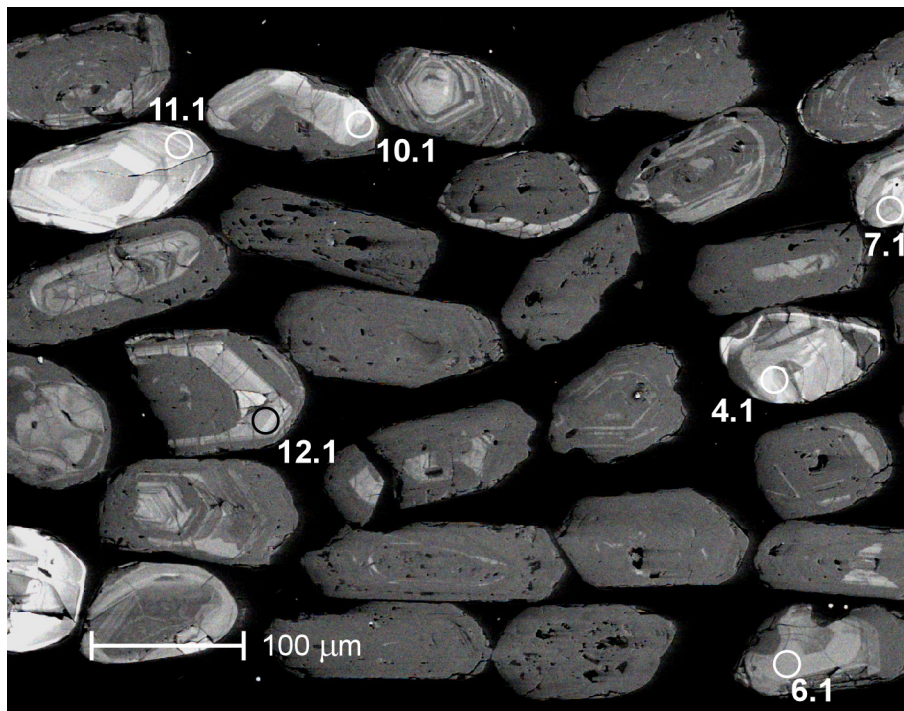


Figure 1. Cathodoluminescence image of representative zircons from sample 213029: quartz–muscovite schist, GD5 Bore. Numbered circles indicate the approximate locations of analysis sites

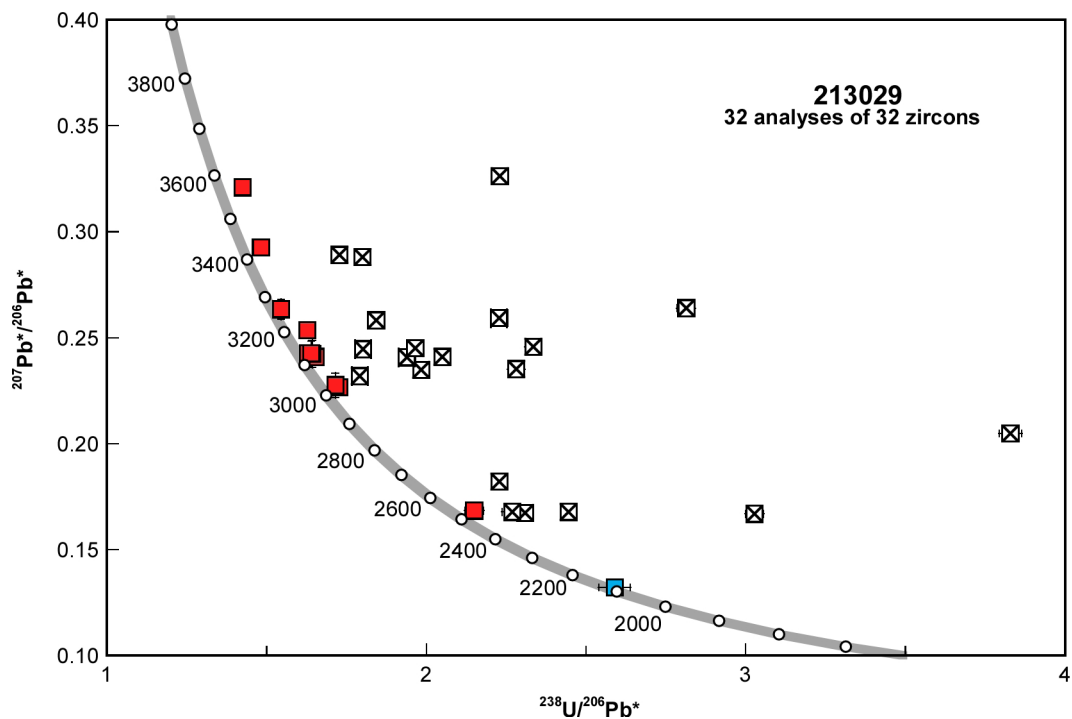
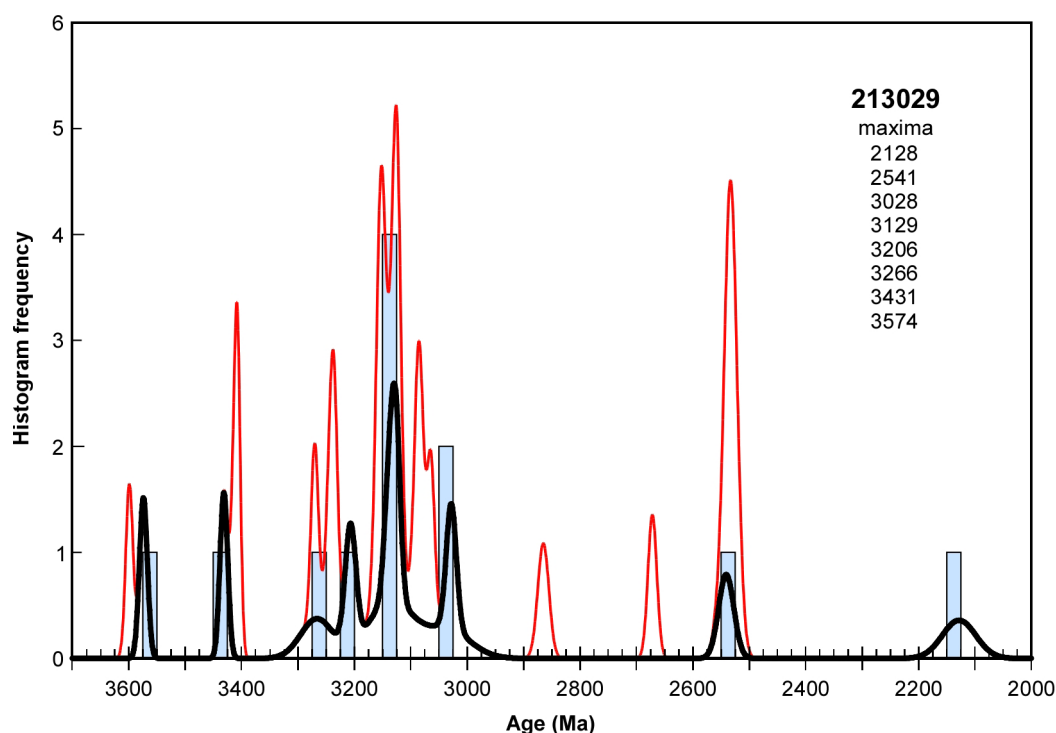


Figure 2. U–Pb analytical data for zircons from sample 213029: quartz–muscovite schist, GD5 Bore. Blue square indicates Group Y (youngest detrital zircon); red squares indicate Group S (older detrital zircons); crossed squares indicate Group D (discordance >5%)

Table 1. Ion microprobe analytical results for zircons from sample 213029: quartz–muscovite schist, GD5 Bore

Group ID	Spot no.	Spot	Grain. spot	<sup>238</sup> U (ppm)	<sup>232</sup> Th (ppm)	<sup>232</sup> Th/ <sup>238</sup> U	f204 (%)	<sup>238</sup> U/ <sup>206</sup> Pb ± 1σ	<sup>207</sup> Pb/ <sup>206</sup> Pb ± 1σ	<sup>238</sup> U/ <sup>206</sup> Pb* ± 1σ	<sup>207</sup> Pb*/ <sup>206</sup> Pb* ± 1σ	<sup>238</sup> U/ <sup>208</sup> Pb* date (Ma) ± 1σ	<sup>207</sup> Pb*/ <sup>208</sup> Pb* date (Ma) ± 1σ	Disc. (%)					
Y	27	27.1	40	26	0.68	-0.404	2.600	0.049	0.12868	0.00172	2.590	0.049	0.13226	0.00224	2105	34	2128	30	1.1
S	2	2.1	79	118	1.55	0.095	2.148	0.029	0.16917	0.00129	2.150	0.029	0.16832	0.00135	2462	28	2541	13	3.1
S	11	11.1	102	137	1.39	0.014	1.727	0.022	0.22673	0.00127	1.727	0.022	0.22661	0.00127	2945	30	3028	9	2.7
S	4	4.1	106	151	1.47	0.065	1.714	0.021	0.22821	0.00574	1.715	0.021	0.22763	0.00575	2961	29	3035	41	2.5
S	22	22.1	183	62	0.35	-0.021	1.655	0.017	0.24067	0.00116	1.654	0.017	0.24086	0.00116	3048	25	3126	8	2.5
S	10	10.1	138	78	0.59	0.009	1.642	0.019	0.24234	0.00634	1.643	0.019	0.24225	0.00634	3065	28	3135	42	2.2
S	14	14.1	93	51	0.56	0.094	1.628	0.021	0.24346	0.00131	1.630	0.021	0.24263	0.00135	3084	32	3137	9	1.7
S	13	13.1	94	35	0.38	-0.014	1.639	0.021	0.24253	0.00576	1.639	0.021	0.24265	0.00576	3071	32	3137	38	2.1
S	17	17.1	81	77	0.98	0.098	1.627	0.022	0.25438	0.00148	1.628	0.022	0.25352	0.00153	3086	34	3207	10	3.8
S	19	19.1	145	117	0.83	0.008	1.546	0.017	0.26337	0.00480	1.546	0.017	0.26330	0.00480	3215	28	3267	29	1.6
S	32	32.1	120	55	0.48	0.009	1.482	0.017	0.29264	0.00128	1.482	0.017	0.29256	0.00129	3324	31	3431	7	3.1
S	24	24.1	95	39	0.42	-0.011	1.424	0.018	0.32076	0.00147	1.424	0.018	0.32085	0.00147	3429	35	3574	7	4.1
D	6	6.1	246	536	2.25	0.285	3.019	0.028	0.16937	0.00089	3.027	0.028	0.16682	0.00102	1840	15	2526	10	27.2
D	7	7.1	167	372	2.30	0.082	2.308	0.024	0.16806	0.00093	2.309	0.024	0.16733	0.00097	2319	20	2531	10	8.4
D	18	18.1	233	405	1.80	0.081	2.443	0.023	0.16854	0.00083	2.445	0.023	0.16782	0.00086	2210	18	2536	9	12.8
D	26	26.1	84	212	2.59	-0.026	2.270	0.031	0.16759	0.00132	2.269	0.031	0.16782	0.00134	2354	27	2536	13	7.2
D	29	29.1	233	254	1.12	0.080	2.227	0.021	0.18279	0.00083	2.229	0.021	0.18207	0.00087	2389	19	2672	8	10.6
D	31	31.1	239	776	3.35	0.358	3.815	0.035	0.20804	0.00105	3.829	0.035	0.20484	0.00124	1496	12	2865	10	47.8
D	21	21.1	185	113	0.63	0.008	1.791	0.018	0.23189	0.00099	1.791	0.018	0.23182	0.00099	2859	24	3065	7	6.7
D	9	9.1	193	317	1.70	0.133	1.981	0.020	0.23595	0.00098	1.984	0.020	0.23476	0.00102	2632	22	3085	7	14.7
D	5	5.1	129	409	3.28	0.176	2.278	0.026	0.23672	0.00133	2.282	0.026	0.23516	0.00141	2343	23	3087	10	24.1
D	12	12.1	189	439	2.40	0.051	1.938	0.020	0.24108	0.00105	1.939	0.020	0.24063	0.00107	2681	23	3124	7	14.2
D	1	1.1	168	290	1.79	0.064	2.049	0.020	0.24143	0.00125	2.050	0.020	0.24087	0.00127	2561	21	3126	8	18.1
D	23	23.1	131	215	1.70	0.055	1.801	0.020	0.24503	0.00120	1.802	0.020	0.24455	0.00122	2846	26	3150	8	9.6
D	8	8.1	159	312	2.03	0.046	1.964	0.021	0.24541	0.00111	1.965	0.021	0.24500	0.00112	2652	23	3153	7	15.9
D	30	30.1	153	399	2.70	0.196	2.330	0.025	0.24741	0.00119	2.335	0.025	0.24568	0.00126	2298	21	3157	8	27.2
D	3	3.1	180	213	1.23	0.070	1.842	0.019	0.25885	0.00107	1.843	0.019	0.25824	0.00109	2794	23	3236	7	13.6
D	15	15.1	127	567	4.60	0.193	2.224	0.025	0.26094	0.00131	2.228	0.025	0.25925	0.00138	2390	23	3242	8	26.3
D	28	28.1	223	855	3.97	0.179	2.809	0.028	0.26550	0.00104	2.814	0.028	0.26393	0.00108	1960	17	3270	6	40.1
D	16	16.1	261	471	1.86	0.080	1.799	0.017	0.28870	0.00094	1.800	0.017	0.28801	0.00095	2848	21	3407	5	16.4
D	20	20.1	167	420	2.60	0.050	1.727	0.018	0.28941	0.00122	1.728	0.018	0.28898	0.00123	2943	25	3412	7	13.7
D	25	25.1	190	1644	8.95	0.227	2.225	0.025	0.32800	0.00133	2.230	0.025	0.32609	0.00138	2388	23	3599	6	33.6



**Figure 3.** Probability density diagram and histogram for sample 213029: quartz–muscovite schist, GD5 Bore. Thick curve, maxima values, and frequency histogram (bin width 25 Ma) include only data with discordance  $< 5\%$  (12 analyses of 12 zircons). Thin curve includes all data (32 analyses of 32 zircons)

Group S comprises 11 analyses (Table 1), which yield  $^{207}\text{Pb}^*/^{206}\text{Pb}^*$  dates of 3574–2541 Ma.

It is possible that all of the analyses in Group Y and S are of unmodified detrital zircons, in which case the date of  $2128 \pm 30$  Ma ( $1\sigma$ ) for the single analysis in Group Y represents a maximum age of deposition for the precursor of muscovite schist. A more conservative estimate of the maximum depositional age can be based on the weighted mean  $^{207}\text{Pb}^*/^{206}\text{Pb}^*$  date of  $3131 \pm 11$  Ma (MSWD = 0.34) for the youngest coherent group of four analyses in Group S.

The data for combined Groups Y and S indicate significant age components at c. 3206 and 3129 Ma (Fig. 3), based on contributions from approximately 3 and 4 analyses, respectively. These age components are interpreted as the ages of zircon-crystallizing rocks in the detrital source regions, or the ages of detrital components within sediments that have been reworked into this rock.

The youngest analysis in Group S, together with four discordant analyses in Group D, yield a weighted mean  $^{207}\text{Pb}^*/^{206}\text{Pb}^*$  date of  $2533 \pm 9$  Ma (MSWD = 0.26), which is similar to the youngest age component identified in a sample of arkosic metasandstone from this locality by Page et al. (1995).

## References

- Blake, DH, Tyler, IM, Warren, RG, 2000, Gordon Downs 1:250 000 Geological Series Sheet SE 52-10 Second Edition, Australian Geological Survey Organisation and Geological Survey of Western Australia, Map, Map Legend.
- Dunster, JN and Ahmad, M 2013, Chapter 17: Birrindudu Basin, in *Geology and Mineral Resources of the Northern Territory*, compiled by M Ahmad and TJ Munson: Northern Territory Geological Survey, Special Publication 5.
- Lu, Y, Wingate, MTD, Morin-Ka, S and Beardsmore, TJ 2017a, 213019: quartz arenite, Kundat Djaru; *Geochronology Record* 1398: Geological Survey of Western Australia, 6p.
- Lu, Y, Wingate, MTD, Morin-Ka, S and Beardsmore, TJ 2017b, 213028: muscovite schist, GD5 Bore; *Geochronology Record* 1399: Geological Survey of Western Australia, 5p.
- Page, R, Sun, SS, Blake, D, Edgecombe, D and Pearcey, D 1995, Geochronology of an exposed late Archean basement terrane in the Granites-Tanami region: *AGSO Research Newsletter*, v.22, p.21–22.
- Stacey, JS and Kramers, JD 1975, Approximation of terrestrial lead isotope evolution by a two-stage model: *Earth and Planetary Science Letters*, v. 26, p. 207–221.

## Recommended reference for this publication

- Lu, Y, Wingate, MTD, Morin-Ka, S and Beardsmore, TJ 2017, 213029: muscovite schist, GD5 Bore; *Geochronology Record* 1400: Geological Survey of Western Australia, 4p.

Data obtained: 13 February 2016

Data released: 28 April 2017